



Minerva Access is the Institutional Repository of The University of Melbourne

Author/s:

Curran, SC;Drăgușin, V;Pobiner, B;Pante, M;Hellstrom, J;Woodhead, J;Croitor, R;Doboș, A;Gogol, SE;Ersek, V;Keevil, TL;Petculescu, A;Popescu, A;Robinson, C;Werdelin, L;Terhune, CE

Title:

Hominin presence in Eurasia by at least 1.95 million years ago

Date:

2025-12-01

Citation:

Curran, S. C., Drăgușin, V., Pobiner, B., Pante, M., Hellstrom, J., Woodhead, J., Croitor, R., Doboș, A., Gogol, S. E., Ersek, V., Keevil, T. L., Petculescu, A., Popescu, A., Robinson, C., Werdelin, L. & Terhune, C. E. (2025). Hominin presence in Eurasia by at least 1.95 million years ago. *Nature Communications*, 16 (1), pp.836-. <https://doi.org/10.1038/s41467-025-56154-9>.

Persistent Link:

<https://hdl.handle.net/11343/359639>

License:

[CC BY-NC-ND](#)

Hominin presence in Eurasia by at least 1.95 million years ago

Received: 3 May 2024

Accepted: 10 January 2025

Published online: 20 January 2025

Check for updates

Sabrina C. Curran ^{1,15}✉, Virgil Drăgușin ², Briana Pobiner ³, Michael Pante⁴, John Hellstrom⁵, Jon Woodhead ⁵, Roman Croitor ⁶, Adrian Doboș⁷, Samantha E. Gogol ⁸, Vasile Ersek ⁹, Trevor L. Keevil⁴, Alexandru Petculescu², Aurelian Popescu¹⁰, Chris Robinson^{11,12}, Lars Werdelin ¹³ & Claire E. Terhune ^{14,15}✉

The timing of the initial dispersal of hominins into Eurasia is unclear. Current evidence indicates hominins were present at Dmanisi, Georgia by 1.8 million years ago (Ma), but other ephemeral traces of hominins across Eurasia predate Dmanisi. However, no hominin remains have been definitively described from Europe until ~1.4 Ma. Here we present evidence of hominin activity at the site of Grăunceanu, Romania in the form of multiple cut-marked bones. Biostratigraphic and high-resolution U-Pb age estimates suggest Grăunceanu is >1.95 Ma, making this site one of the best-dated early hominin localities in Europe. Environmental reconstructions based on isotopic analyses of horse dentition suggest Grăunceanu would have been relatively temperate and seasonal, demonstrating a wide habitat tolerance in even the earliest hominins in Eurasia. Our results, presented along with multiple other lines of evidence, point to a widespread, though perhaps intermittent, presence of hominins across Eurasia by at least 2.0 Ma.

Current evidence for the earliest appearance of hominins outside Africa comes from the site of Dmanisi, Georgia. Dated to 1.85–1.77 Ma¹, the Dmanisi assemblage includes a large number of hominin remains², as well as lithics and evidence of hominin modification of animal remains (e.g., butchery marks³). This site clearly demonstrates a hominin presence in Southwest Asia/Eastern Europe by the Early Pleistocene (Gelasian), yet the exact timing of the initial dispersal of hominins out of Africa and the long-term success of these dispersals is debated (e.g.,⁴). This is especially true for Europe, where there is an ongoing discourse regarding the timing of hominin presence in

southern and northern Europe^{5,6}. Updated chronologies for fossil localities in Asia (especially China⁷) and a growing number of localities that may represent fleeting or ephemeral traces of hominin activity (e.g., lithics and/or anthropogenic modifications of bones unaccompanied by hominin fossils) throughout Eurasia increasingly suggest hominins were likely present in Eurasia prior to Dmanisi (Fig. 1).

One Early Pleistocene Eurasian locality that could shed light on the initial dispersal of hominins into Eurasia is Grăunceanu, located in the Olteț River Valley (ORV) of Romania. This region is situated in the

¹Department of Sociology & Anthropology, Ohio University; Athens, Ohio, USA. ²Emil Racoviță Institute of Speleology, Romanian Academy, Bucharest, Romania. ³Department of Anthropology, Smithsonian Institution, Washington, DC, USA. ⁴Department of Anthropology and Geography, Colorado State University, Fort Collins, CO, USA. ⁵School of Geography, Earth and Atmospheric Sciences, University of Melbourne, Melbourne, Australia. ⁶Institute of Zoology, Moldova State University, Chișinău, Republic of Moldova. ⁷Department of Paleolithic Archaeology, Vasile Pârvan Institute of Archaeology, Romanian Academy, Bucharest, Romania. ⁸Department of Anthropology, University of Minnesota, Minneapolis, MN, USA. ⁹Department of Geography and Environmental Sciences, Northumbria University, Newcastle-upon-Tyne, United Kingdom. ¹⁰Museum of Oltenia, Craiova, Romania. ¹¹Department of Biological Sciences, Bronx Community College, New York, NY, USA. ¹²Department of Anthropology, The Graduate Center, City University of New York, New York, NY, USA. ¹³Department of Paleozoology, Swedish Museum of Natural History, Stockholm, Sweden. ¹⁴Department of Anthropology, University of Arkansas, Fayetteville, AR, USA. ¹⁵These authors contributed equally: Sabrina C. Curran, Claire E. Terhune. ✉e-mail: currans@ohio.edu; cterhune@uark.edu

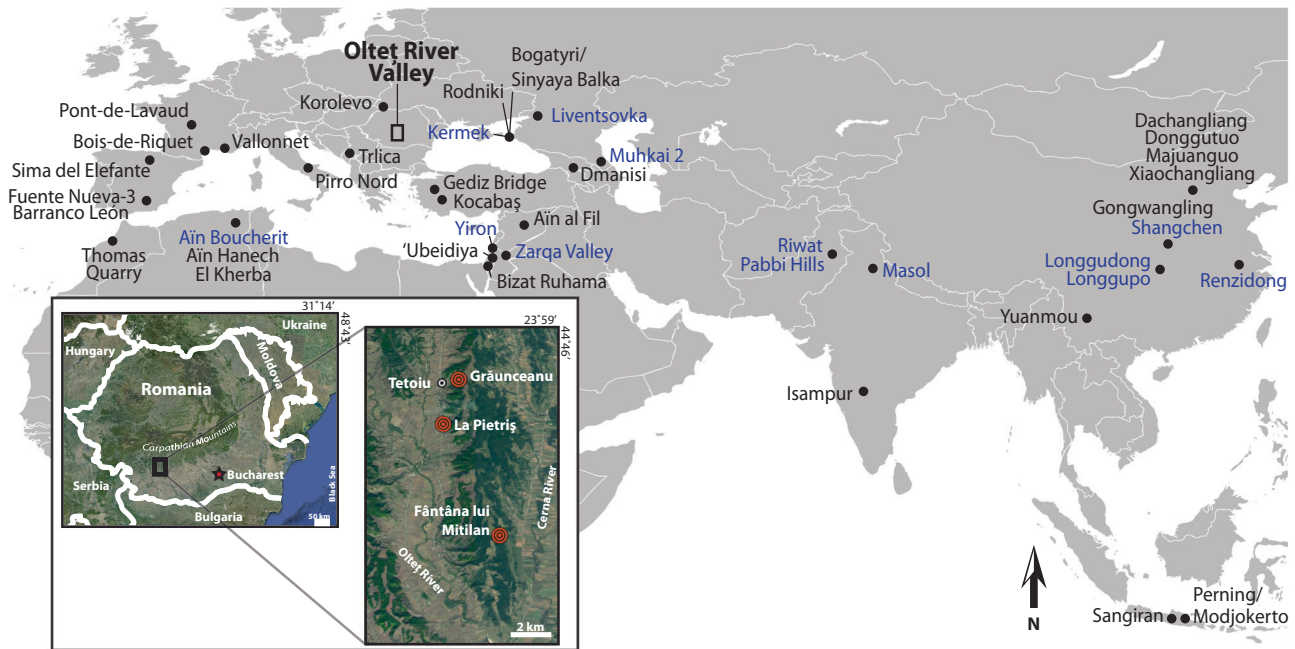


Fig. 1 | Map of fossil localities showing evidence of hominins (either hominin fossils, lithics, or cut-marked bones) in northern Africa and Eurasia prior to 1.0 Ma. Sites shown in blue text are suggested to be > 2 Ma. Inset in the lower left corner shows locations of fossil sites discussed in this study. Citations for fossil localities are provided in Supplementary Data 4. Blank world map data with country

borders was drawn from Wikimedia Commons (CC-BY-SA 3.0). Map inset images are drawn from satellite imagery available via Google Earth (GoogleLandsat / CopernicusData SIO, NOAA, U.S. Navy, NGA, GEBCOGeoBasis-DE/BKG ©2009 and GoogleAirbusMaxar TechnologiesCNES / Airbus).

Dacian sedimentary basin, just south of the Carpathian Mountains (Fig. 1). Deposits stem from the Tetoiu Formation, sediments of which represent multiple fluvio-lacustrine sequences that are rich in fossils^{8,9}. This formation extends from the base of the Pleistocene to as young as ~1.3 Ma⁸ (see Supplementary Note 1). Grăunceanu was originally excavated in the 1960s and is one of the best known Early Pleistocene sites from East-Central Europe. Biochronological assessments indicate Grăunceanu is Late Villafranchian (~2.2–1.9 Ma) and is attributed to mammalian biostratigraphic zones MN17/MmQ1^{9–11}. At least 31 taxa (Supplementary Data 1) are identified from Grăunceanu, including mammoth, multiple species of bovids and cervids, giraffids, equids, rhinocerotids, multiple carnivore species, rodents (beaver, porcupine), ostrich, a large species of terrestrial monkey (*Paradolichopithecus*), and the youngest representative of pangolins in Europe^{11–14}. Paleoeological analyses suggest Grăunceanu was a forest-steppe environment along the paleo-Oltet river¹⁵. Other localities in the ORV include the penecontemporaneous sites of La Pietriș and Valea Roșcâi and the slightly biochronologically younger Fântâna lui Mitilan⁹, as well as multiple smaller localities. Though no hominin remains or in situ lithics have been identified from Grăunceanu, prior researchers have described lithics (see Supplementary Note 2 and Supplementary Fig. 1) from the nearby penecontemporaneous site of Dealul Mijlociu¹⁶, which Radulesco and Samson⁹ placed in a similar faunal horizon as Grăunceanu based on their biochronological comparisons.

Here we present evidence of hominin presence in Eurasia by at least 1.95 Ma in the form of cut-marked bones from the site of Grăunceanu, Romania, supported by high-precision uranium-lead (U-Pb) age estimates. We also perform high-resolution oxygen and carbon stable isotope analysis of a horse maxilla from the same site to reconstruct temperature seasonality and precipitation. We place these data into the context of the larger discussion regarding ephemeral traces of early hominin dispersals into Eurasia in the Early Pleistocene and argue in favor of a hominin presence across Eurasia by at least 2.0 Ma.

Results

Taphonomy

The total number of identified specimens (NISP) from Grăunceanu is 4983. Of these, 4524 (excluding isolated teeth and horn/antler specimens) were examined under strong, low-angled light for evidence of bone surface modifications (BSMs) by one or more observers, following protocols outlined in ref. 17. The taphonomic condition of the remains is very consistent (i.e., all bones show similar coloration and post-depositional alterations), with many bones still in articulation at the time of excavation, and the majority of specimens (> 75%) preserving at least half of the original skeletal element. We interpret this assemblage as representing a single deposition, likely a low-energy overbank seasonal flood deposit. The assemblage overall shows little weathering (85.3% of specimens at weathering stage 0) or water-based alterations (only 21 specimens have polishing). These results suggest the assemblage was not subject to reworking and was not exposed for long on the surface before burial. Bone surface visibility overall is very good, with most specimens (> 73%) having 75–100% of the bone surface visible. A large proportion of specimens (81.7%) present some degree of root-etching, and post-depositional damage (e.g., chipping, cracking, exfoliation, etc.) was present on 41.5% of specimens. Carnivore damage is present on 9.5% of the assemblage in the form of tooth scores, pits, crenulated break edges, or any combination of these three bone modifications.

A total of 1,189 specimens from Grăunceanu exhibit linear marks; the vast majority of these were identified as tooth ($n = 290$), trampling ($n = 172$), excavator ($n = 296$), or unknown ($n = 411$) marks (see Supplementary Notes 3–5). No evidence of percussion marks was recorded. Twenty specimens total exhibit cut marks; of these, 7 display high-confidence cut marks, 12 show probable cut marks, and 1 specimen presents both types of marks (Fig. 2, Supplementary Figs. 2–21, Supplementary Data 2); detailed descriptions of all marks can be found in Supplementary Note 5. Cut marks were identified using two methods: 1) qualitative analyses modified from^{18,19}, and 2) quantitative analyses using methods outlined in ref. 20

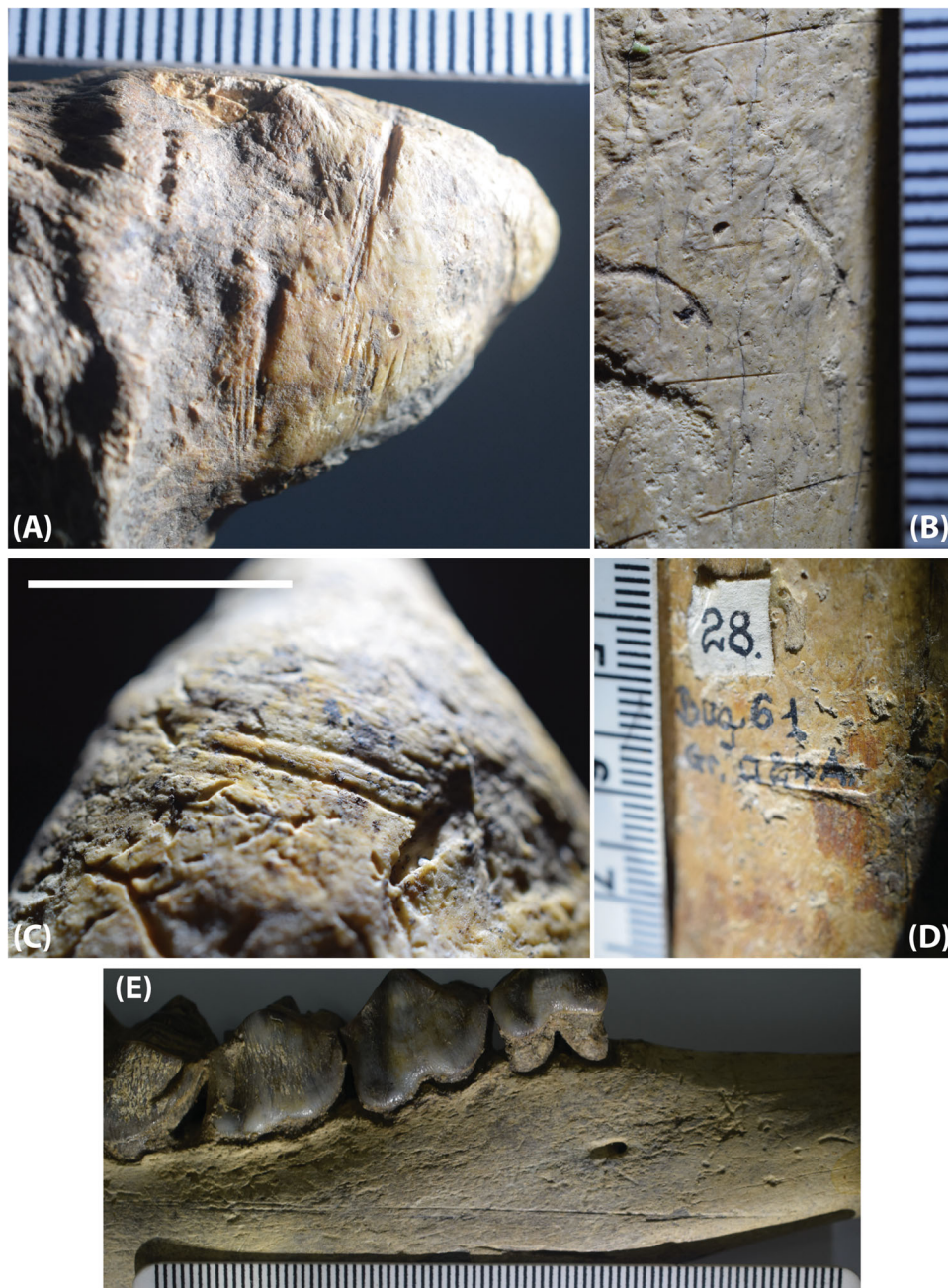


Fig. 2 | Selected images of high-confidence cut-marked specimens from the Olteț River Valley assemblage. A = VGr.1483, B = VGr.2004, C = VGr.1515, D = VGr.0519, E = FM.0091. Scale bar in C is 1 cm.

(Supplementary Figs. 22–24, Supplementary Table 1). The eight specimens identified as having high-confidence cut marks include four tibiae, one mandible, one humerus, and two long bone fragments. All of the taxonomically identifiable specimens with high-confidence cut marks are from artiodactyls, except one small carnivorous tibia. Most specimens have two or more linear marks identified as cut marks. All high-confidence cut marks have straight trajectories, primarily transverse orientations relative to the long axis of the bone, and the same color within the mark as the main bone surface, while very few have preserved evidence of microstriations or shoulder effects. For specimens that could be identified to element, the cut marks appear in anatomical locations consistent with defleshing, especially the distal tibia. Most marks identified as high-confidence cut marks were also classified as cut marks by the

quantitative analysis with high posterior probabilities (Supplementary Data 2).

The 13 specimens exhibiting probable cut marks were given lower confidence due to these specimens having more degraded surfaces (e.g., root etching, surface exfoliation), not being identified as cut marks in the quantitative analysis, and/or not presenting enough qualitative features to be definitively identified as cut marks. These marks are found on a wider variety of skeletal elements, though metapodia are the most frequent ($n = 5$), followed by other long bones and mandibles. Probable cut marks could be a single long linear mark or a patch of up to 15 small linear marks. Most have straight trajectories, are more frequently obliquely oriented to the long axis of the bone, rarely have microstriations, and none exhibit shoulder effects.

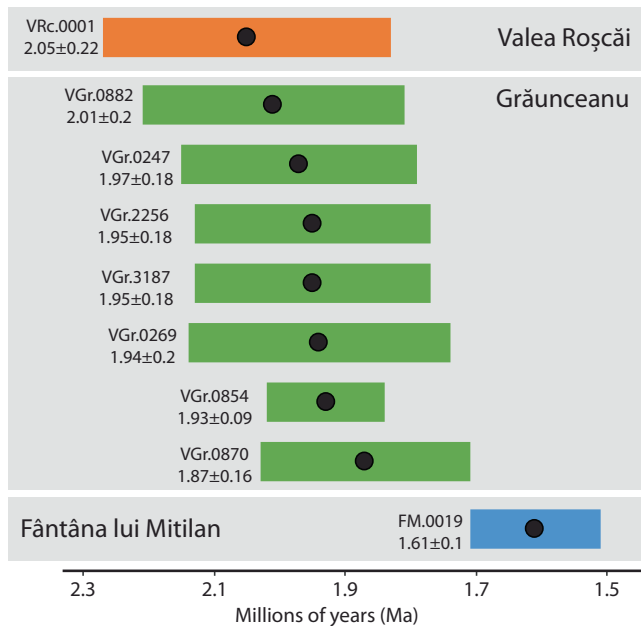


Fig. 3 | Results of the U-Pb dating analysis. Results show age per sample (black circles) with corresponding uncertainties ($\pm 2\sigma$) after corrections accounting for initial ^{238}U - ^{234}U disequilibrium for the nine samples from three localities analyzed here. See Supplementary Table 2 for details of each sample.

U-Pb dating

Radiometric ages for ORV localities were estimated using laser ablation U-Pb analyses (broadly following²¹ and parameters detailed in Supplementary Table 2) of dentine from seven mammal specimens from Grăunceanu, one from Valea Roșcăi, and one from Fântâna lui Mitilan (Fig. 3, Supplementary Tables 3 and 4, Supplementary Figs. 25 and 26). In Supplementary Table 5 we show both “equilibrium” age estimates, based on the U-Pb data, and also slightly younger “disequilibrium-corrected” ages, which take into consideration potential initial disequilibrium in the ^{238}U - ^{206}Pb decay chain (see Supplementary Note 6). All subsequent discussion utilizes the latter, which provide the most robust age estimates for the Grăunceanu samples and range from 2.01 ± 0.20 Ma to 1.87 ± 0.16 Ma ($\pm 2\sigma$) with an average of 1.95 Ma; ages cluster tightly around this average (Fig. 3), lending high confidence to this estimate. Specimen VRc.0001 from Valea Roșcăi returned a corrected age of 2.05 ± 0.22 Ma, while specimen FM.0019 from Fântâna lui Mitilan returned a corrected age of 1.61 ± 0.10 Ma. These U-Pb estimates agree with biochronological estimates for Grăunceanu and Fântâna lui Mitilan¹¹ and with the stratigraphic positioning of Valea Roșcăi, which has been suggested to be similar in age to Grăunceanu⁹ (see Supplementary Note 6). These results provide our best estimates of the minimum ages of fossil burial, as they represent final closure of the U-Pb system following post-depositional uranium exchange with the environment, which is ubiquitous in fossil teeth and bone samples. The time between deposition and closure is almost certainly variable and probably site related. These U-Pb results, coupled with the biochronology for these localities^{11–14}, lend high confidence to our estimated age of deposition for Grăunceanu of >1.95 Ma and potentially prior to 2.0 Ma, and indicate that Grăunceanu may be the earliest locality in Europe to show evidence for hominin activity.

Stable isotopes

We analyzed oxygen ($\delta^{18}\text{O}$) and carbon ($\delta^{13}\text{C}$) stable isotope ratios from post-weaning cheek teeth of an *Equus* sp. specimen from Grăunceanu (Fig. 4, Supplementary Data 3, Supplementary Note 7). We used high-resolution sampling to assess variation across the tooth crown and

along the tooth row ($\text{P}^2\text{-M}^3$); this allowed us to examine seasonal fluctuations in rainfall, as equids are obligate drinkers (i.e., they depend on fresh water sources) and their diet is relatively fixed (i.e., grazing).

The $\delta^{18}\text{O}$ values we observe in carbonate vary between 19.9‰ and 26.2‰ (Vienna Standard Mean Ocean Water; VSMOW), with an average value of 23.5‰. Curran et al.¹⁵ reported mean $\delta^{18}\text{O}$ values from Grăunceanu of 18.9‰ to 25.3‰ (VSMOW) and this slight difference could be explained by the fact that their values were measured on bulk samples from multiple artiodactyl specimens, incorporating enamel with an undetermined seasonal bias, or could represent variation in feeding behaviors and/or migratory habits.

We converted these $\delta^{18}\text{O}$ isotopic values to meteoric water values using three different transfer functions^{22–24}. The average of annual values across the P2-P3-P4-M3 tooth series and across the three equations is -10.8 ± 1.0 ‰ (VSMOW), which is lower than the present-day weighted mean at Râmnicu Vâlcea of -8.1 ‰. Such a large difference would result in annual temperature reconstructions of -4 °C if the equations of Rozanski et al.²⁵ or Pryor et al.²⁶ were employed, but this reconstruction is incompatible with the presence of warm-adapted fauna at Grăunceanu^{13–15}. Multiple factors could influence the isotopic signature of rainfall at Grăunceanu (e.g., air mass origin, rain-out history, global ice volume, moisture recycling); however, information on these factors from the Early Pleistocene is scarce and does not allow us to discuss their potential isotopic impact on regional rainfall. Thus, we argue that this lower value suggests an increased winter precipitation component to aquifer recharge compared to present. An increased winter component in the Early Pleistocene could also explain why reconstructed summer values at Grăunceanu (-7.3 ‰) are lower than regional values for today²⁷ (-3.9 ‰), as the horse might have consumed water with a stronger winter isotopic signal (see Supplementary Note 7).

Conversion of our enamel $\delta^{13}\text{C}$ values to plant tissue $\delta^{13}\text{C}$ yields values between -28.9 ± 0.5 ‰ and -25.7 ± 0.5 ‰ (VPDB), consistent with feeding in a woodland to woodland-mesic C3 grassland²⁸, and supports prior environmental reconstructions for Grăunceanu¹⁵. The highest values are recorded in summer, which could be related to photosynthesis under drought stress²⁹, while the lowest values are recorded during winter (Fig. 4). Using the equation of Kohn²⁹ and after performing full error propagation, we obtained precipitation values between -4 and 32 mm for the driest month, and between 45–222 mm for the wettest month. This result further supports our interpretation of an increased winter precipitation component to aquifer recharge in the ORV.

Discussion

The ongoing debate regarding the timing and location of the earliest hominin dispersal(s) into Eurasia has been hampered by a variety of challenges, including dating uncertainty, lack of research in some geographic regions, and arguments about the anthropogenic nature of several lithic assemblages^{5,30}. A survey of reported early hominin sites in Eurasia and northern Africa >1 Ma (Figs. 1, 5) returns at least 49 localities spread across these regions; 16 potentially predate Dmanisi. The sites show a combination of hominin fossils, lithic assemblages, and evidence of butchery, though only a few include all three indicators.

The earliest sites (pre-2 Ma) outside of Africa cluster in the Middle East, western Russia around the Black and Caspian Seas, central Asia, and China. These sites include a mixture of localities with only lithics and/or a small number of bones with cut marks. Several sites in this group have been reported to have cut-marked bones, though the percentages of the assemblages showing these modifications is low (Masol= three cut-marked bones³¹, Liventsovka= one bone with multiple marks³², Muhkai 2= one bone with six marks³³). The only site pre-dating Dmanisi with potential hominin remains is Longgudong at 2.01–1.87 Ma, where six hominin teeth and a large lithic assemblage have been described³⁴.

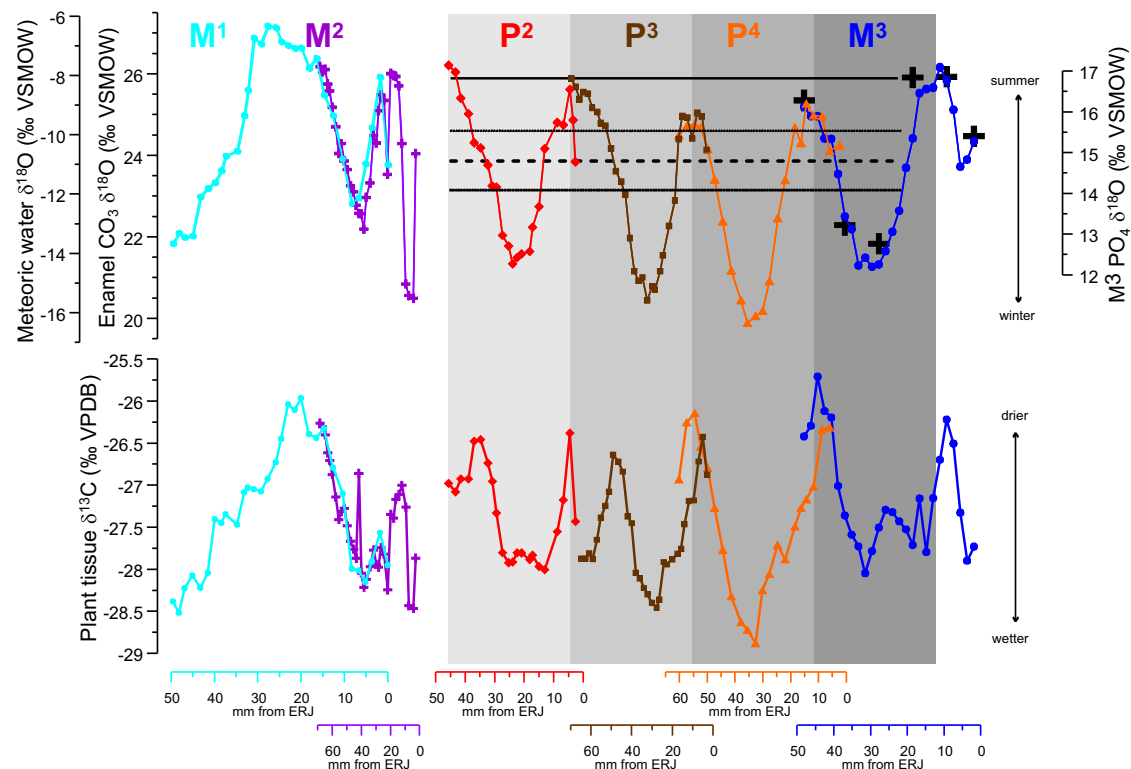


Fig. 4 | Stable oxygen (upper row) and carbon (lower row) isotope values of upper cheek teeth of specimen VGr.0974 assigned to *Equus* sp. Distance is measured from the enamel-root junction (ERJ) in millimeters (mm). The tooth series is arranged according to the eruption and mineralization pattern described in modern horses by ref. 75; M¹= upper first molar, M²= upper second molar, P²= upper second premolar, P³= upper third premolar, P⁴= upper fourth premolar, M³= upper third molar. Black crosses indicate $\delta^{18}O$ values in phosphate samples. M¹ and M² were not used in the climate reconstruction because they represent pre-weaning

values but are figured for comparative reasons. The horizontal solid line represents the modern day weighted average $\delta^{18}O$ value of meteoric water at Râmnicu Vâlcea while the horizontal dashed line and brackets above and below represents the average annual $\delta^{18}O$ value of meteoric water reconstructed for Grăunceanu based on enamel carbonate $\delta^{18}O$. Vertical gray shading represents a year (summer peak to summer peak) for each tooth (see Supplementary Note 7). VSMOW= Vienna Standard Mean Ocean Water; VPDB= Vienna Pee Dee Belemnite. Data represented in this figure are provided in Supplementary Data 3.

Another -dozen sites date to 2–1.5 Ma; these sites are again clustered in the Middle East, Russia, and China and include the first indisputable evidence of hominins outside of Africa (i.e., Dmanisi, Gongwangling). From 1.5 to 1 Ma are the first sites suggesting the presence of hominins in Europe and far southeast Asia; notably these sites show indisputable evidence of hominins in the form of hominin fossils, well-defined lithic assemblages, and a much larger number of sites with animal bones showing evidence of butchery. At present, the earliest hominin fossils from Europe are Barranco León, Spain (1.4 Ma)³⁵, Kocabaş, Turkey (1.3–1.1 Ma)³⁶, and Sima del Elefante, Spain (1.2–1.1 Ma)³⁷, though multiple other localities have lithic assemblages and cut marked faunal remains (Fig. 5).

Cut-marked faunal remains are reported for 21 of the sites listed in Fig. 5. Sites with the highest percentages of the assemblage showing cut marks (Supplementary Table 5) are El Kherba (2.100%³⁸), Aïn Boucherit (Lw) (5.743%³⁹), and Sima del Elefante (5.000%⁴⁰); all other sites report rates of < 2%, sometimes substantially so. At Dmanisi only 0.392% of the assemblage is cut-marked³, demonstrating that evidence for butchery in the assemblage is low, even while hominins were clearly present. In comparison, 0.176% of the Grăunceanu assemblage displays high-confidence cut marks, or 0.442% if probable cut marks are included. Though no lithics or hominin fossils are found at Grăunceanu, our detailed taphonomic analysis reveals clear evidence of hominin presence in the form of anthropogenic bone surface modifications at rates comparable to similarly aged and even younger sites where hominins and/or stone tools are present and well-accepted. While not all sites listed here have published taphonomic assessments, all that have full taphonomic analyses report the presence of cut marks

in their assemblages (Supplementary Table 5). This pattern exists independent of the size of the fossil assemblage and may be a type of “Olduvai Effect”⁴¹, where more intense research leads to more extensive and nuanced interpretations. Thus, it is likely that with further taphonomic investigations, more traces of early hominin presence in Eurasia will be identified.

We recognize that without lithics or hominin fossils from Grăunceanu our taphonomic analysis may be viewed with skepticism. However, there are several Early Pleistocene sites in eastern Africa with published evidence for hominin butchery marks that also do not preserve lithics or hominin fossils^{42–44}. Acknowledging this limitation, we used both established qualitative methods^{18,19} and quantitative methods²⁰ that yield high reclassification rates. The linear marks we identified as cut marks in our qualitative analysis returned high posterior probabilities in the quantitative analysis, supporting their classification. We also conservatively eliminated many linear marks of unknown origin from further consideration. Still, we are left with strong evidence for hominin butchery at Grăunceanu, the strength of which cannot easily be dismissed.

The anthropogenic origin of some of the sites included here, especially those > 2 Ma, are debated^{5,30}. It is possible that some of these sites are incorrectly dated and/or not anthropogenic in origin; however, it is difficult and perhaps unwise to discount this volume of evidence, and we suggest it is prudent to seriously consider that hominins were present in Eurasia prior to 2 Ma. Indeed, our results indicate the presence of hominins in East-Central Europe by ≥ 1.95 Ma. In fact, among European sites potentially older than 2.0 Ma, Grăunceanu stands out as benefitting from the most reliable

estimate of its (minimum) age, with previously published biochronological estimates^{9,11} now supported by radiometric dating that have the analytical advantage of providing associated quantifications of uncertainty.

We purposefully avoid discussion of the hominin species (or multiple species) that may have been the first to disperse into Eurasia. This is a period when multiple hominin species coexisted at sites in eastern and southern Africa^{45,46}. The taxonomic affinity of nearly all hominin fossils in Fig. 5 is debated; many are identified only to *Homo* sp. and others are identified as *Homo erectus/ergaster*. Present evidence^{46,47} indicates that the earliest *H. erectus sensu lato* was present in both South Africa and Ethiopia ca. 2.0 Ma; this therefore broaches the possibility that, if hominins were present in Eurasia prior to 2.0 Ma, then they may not have been *H. erectus*, and/or that *H. erectus* is older than we currently have data for.

There are many uncertainties regarding the initial dispersal of hominins into Eurasia, including timing, routes, and continuity of these dispersals^{4,48}. If hominins initially dispersed out of Africa >2 Ma, then almost certainly the ephemeral nature of their traces is evidence of spatially and/or temporally discontinuous populations, perhaps limited to a restricted latitudinal range and/or interglacial periods where environments may have been more conducive to their presence^{4,49}. There is currently little evidence to support dispersal directly from Africa into Europe via Gibraltar; instead, dates of suggested hominin localities in the Middle East more strongly support dispersal via the Sinai Peninsula⁵⁰ (Fig. 5), though the lack of investigation in some geographic regions makes identifying specific routes challenging. During the Early Pleistocene, the extent of the Black Sea was similar to present-day, implying a similar configuration of its shores, and that it was disconnected from the Mediterranean⁵¹. Thus hominins could have either dispersed from the north around the Black Sea and south into Romania, as suggested by the presence of multiple potential hominin localities in the Caucasus and southwestern Russia⁴⁹, or they may have crossed into Europe via the land bridge between Anatolia and the Balkan peninsula and then dispersed northward, perhaps skirting the shore of the Black Sea.

In any scenario, hominins likely had to contend with cooler environments with more seasonal temperature fluctuations than they would have been adapted to in Africa. Hominin artifacts on the Chinese Loess plateau at 2.12 Ma that were deposited during colder and drier periods suggest hominins were capable of handling cooler climates at this time⁷. Our paleoenvironmental data for Grăunceanu indicate an open, arid environment with some nearby woodlands and water sources¹⁵. However, the presence of more warm-adapted (or at least likely not cold-tolerant) species such as the large terrestrial macaque *Paradolichopithecus*, pangolins, and ostriches suggests that ORV winter temperatures were relatively mild. While fauna indicates mild winters, stable isotope data indicate that precipitation at Grăunceanu had a marked seasonal distribution, likely resulting in wet winters and dry summers. These paleoenvironmental and isotopic results, coupled with the fact that the ORV is situated at ~45° N, support arguments^{4,49} that hominins likely exploited warmer interglacial periods to disperse into higher latitudes (> 40°).

Hominins as a whole, and particularly members of the genus *Homo*, are often characterized by their environmental flexibility⁵². The widespread presence of hominins in Eurasia circa 2 Ma, as we argue and provide evidence for here in the form of cut-marked bones securely dated to minimally 1.95 Ma, is further support for this flexibility. These hominins would have had to contend with new environments and ecosystems with increased seasonality. While it is clear that the hominin presence in Eurasia at this time was likely geographically and temporally discontinuous, the preponderance of ephemeral traces for hominins in this region can no longer be ignored.

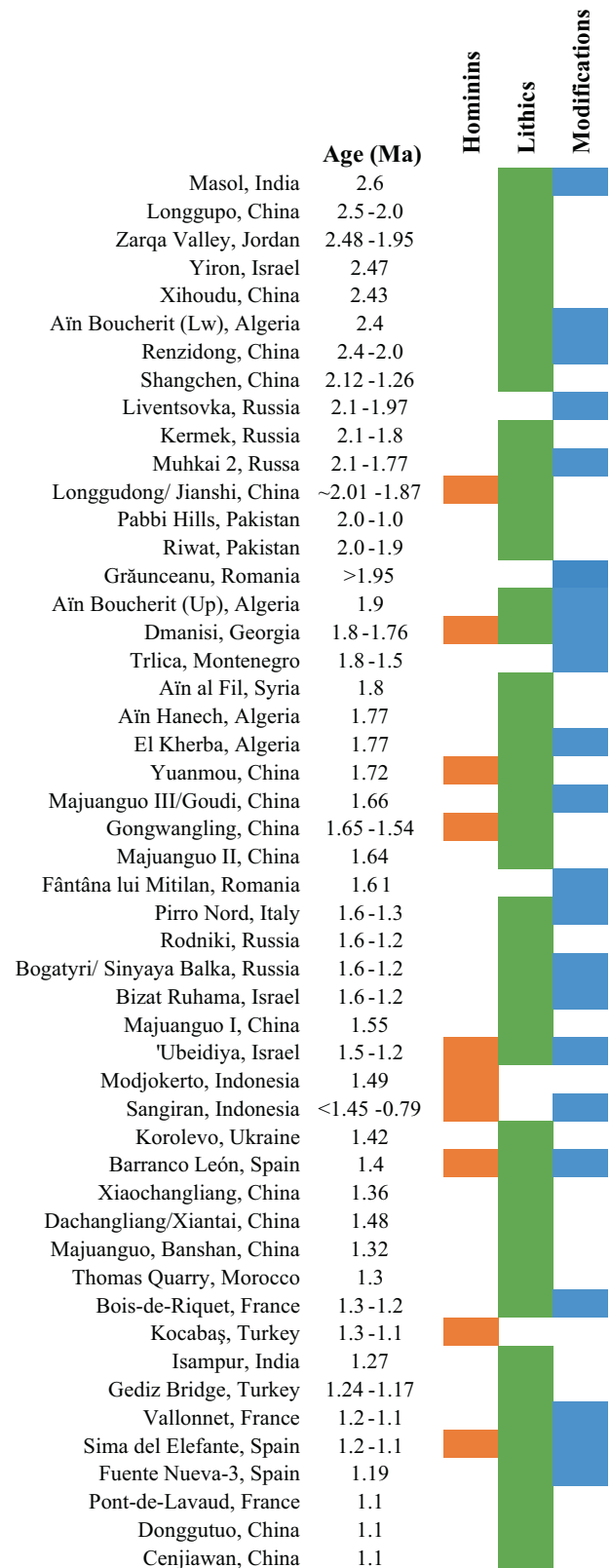


Fig. 5 | Reported hominin localities from the Early Pleistocene of Eurasia and northern Africa prior to 1 Ma. The presence of hominin remains, lithic materials, and hominin modifications (e.g., evidence of butchering) is indicated for each site. See Supplementary Data 4 for associated references and more details for each locality.

Methods

Materials examined as part of this research are housed at the “Emil Racoviță” Institute of Speleology (ISER) and the Museum of Oltenia (MO); materials from the ORV are currently split between these two institutions. These collections are curated by coauthors Petculescu (ISER) and Popescu (MO) and permissions to access the collections for this research were granted by the curators and associated institutions.

Excavations at Grăunceanu were undertaken from 1960–1966, with some additional test excavations and/or collection as early as 1959 and as late as the 1970s. Nearly all excavation records and provenience data have unfortunately been lost. Publications by Bolomey¹⁰ and Radulesco and Samson⁹ describe the open-air site of Grăunceanu as a ~0.75 meter (m) thick bone bed spread over an area 90m², with little to no stratification of the fossil horizon. All Grăunceanu materials examined as part of this study, including those sampled for U-Pb dating and isotopic analysis, come from the original excavations that took place in the 1960s and stem from this single faunal accumulation. We therefore have high confidence that these remains all represent the same depositional event. Detailed taphonomic descriptions of the ORV localities are forthcoming.

Our team has successfully reidentified the locations of multiple of the fossil localities in the ORV, and we have accessioned and/or inventoried these collections. The total number of identified specimens (NISP) for the Olteț River Valley Assemblage is currently 5527. This includes materials from Grăunceanu (NISP = 4983) and smaller localities such as Fântâna lui Mitilan (NISP = 139) and La Pietriș (NISP = 116) (Supplementary Data 1). There are at least 31 unique taxa from Grăunceanu^{11–14}; paleoecological reconstructions¹⁵ suggest Grăunceanu was likely an open grassland environment with some woodlands and water sources nearby, comparable to a forest-steppe habitat.

Qualitative analysis of bone surface modifications

We analyzed a total of 4746 specimens from four localities (Grăunceanu = 4524, La Pietriș = 114, Fântâna lui Mitilan = 68, and Fântâna Alortetei = 40). Specimens were examined for bone surface modifications (BSMs) under strong, low-angled light from a gooseneck lamp both macroscopically and with a 10x hand-lens by one of four analysts (SC, BP, SG, CET) following procedures outlined in ref. 17, in constant consultation with each other. Analyses took place during the summers of 2019 and 2022. Fossil surfaces were inspected for a variety of abiotic (e.g., adhering matrix, smoothing, bone surface pitting, erosion/dissolution, cracking/sediment splitting, exfoliation/flaking) and biotic (carnivore or hominin modification, trampling, root/fungal rhizomorph etching, rodent gnawing, insect activity, digestion, preparator marks) modifications and all instances were recorded in a shared Excel spreadsheet. Linear marks, defined as any mark at least twice as long as it is wide, were given particular attention. For any marks we suspected to be cut marks we recorded a subset of the qualitative criteria established in Domínguez-Rodrigo et al.^{18,19}: trajectory, presence of barbs, orientation, cross-sectional morphology, number of visible marks, internal symmetry, any shoulder effects visible, any microstriations visible inside the linear mark, any other striations outside of the mark, and color of the interior of the mark relative to the rest of the bone surface. Taxonomic identification, skeletal element, side, portion of element present, and anatomical location of the linear mark (when possible) were recorded. Linear marks of suspected anthropogenic origin were photographed using a DSLR with a macro-lens and a Dino-lite Model Edge and molded two to three times using Coltene President Jet light body dental molding material for further quantitative analysis as described below.

Quantitative analyzes of bone surface modifications. Impressions were taken of marks observed during the qualitative analysis using Coltene President Jet light body dental molding material and sent to MP for quantitative analysis. Marks of interest were molded several

times, and the second set of molds were used in this analysis, since adhering sediment on some specimens was removed in the first round of molding. Because all materials are completely mineralized the molding process did not damage or alter the surface of the bones. MP was kept blind to the results of the qualitative analysis and no other contextual information was provided. Photographic images were only shared after the initial analysis when it became clear that some marks analyzed by MP were not the mark intended for study. These were removed from the analysis and in most cases the correct mark was subsequently identified on the mold and analyzed. In some cases, the mark intended for study was not present or was poorly preserved in the mold, and in a few instances marks that were molded correctly were subsequently removed from analysis due to bioerosion overlapping a portion of the mark.

Quantitative analysis of BSMs from Grăunceanu followed the protocol presented in Pante et al.²⁰. 3D models were created directly from molds using a S Neox 3D optical profilometer (manufactured in 2018) located in the 3D imaging and analysis lab at Colorado State University. All models were produced using a 5x lens that has a z axis resolution of 75 nm. The 5x lens has a numerical aperture of 0.15, a working distance of 23.5 mm, a field of view of 3400 μm x 2837 μm, a spatial sampling of 2.76 μm, and an optical resolution of 0.93 μm. The spatial resolution exceeds that of the Nanovea ST400 white-light non-contact confocal profilometer used in Pante et al.²⁰ which sampled at 5 μm and 10 μm respectively. However, the z-resolution of 40 nm is slightly higher on the Nanovea profilometer. The scale of these resolution differences does not significantly impact our analysis because they are orders of magnitude smaller than the scale of the measured differences between mark types. Further, these differences are smaller than the reported variability in measurements taken from a single mark using the same instrument (Pante et al.²⁰). Processing and analysis of 3D models was carried out using Digital Surf's Mountains® following Pante et al.²⁰. Processing included removing outliers, filling in missing data points, and removing the underlying form of the bone with the mark excluded from the form removal process (See Pante et al.²⁰ for further detail). Data collected through the analysis from the entire 3D model of the BSM were volume, surface area, maximum depth, mean depth, maximum length, and maximum width. Additional data were collected from a profile taken from the deepest point of the BSM including area of the hole, depth of the profile, width, roughness (Ra), opening angle, and radius of the hole.

Fossil data were then statistically compared with a sample of 898 BSMs of known origin, including: 405 cut marks from a variety of stone tool types and raw materials⁵³; 275 tooth marks from crocodiles and five species of mammalian carnivores⁵⁴; 130 trample marks produced by cows on substrates including sand, gravel, and soil⁵⁵; and 88 percussion marks from both anvils and hammerstones⁵⁶. Surface area and depth of the profile were excluded from the statistical analyses because they are redundant with measurements of volume and maximum depth, respectively. All experimental data were transformed using the Box-Cox method to normalize the distributions for each variable and the same transformations were applied to the archeological data. Fossil mark classifications were carried out using the quadratic discriminant analysis function from the MASS package⁵⁷ in R (version 4.4.1); this method was chosen over a linear discriminant analysis because of unequal covariance matrices and sample sizes in our dataset (following Friedman⁵⁸). The accuracy of the QDA model in correctly classifying the experimental BSMs was determined to be 81.4% with 10-fold and 82% with leave-one-out cross-validations performed in R⁵⁹ (version 4.4.1) (Supplementary Table 1). Sensitivity values for true positivity, determined using JMP® statistical software (Version 17), range from 0.91–0.99 indicating the model is very successful at classifying all four types of BSMs (see Supplementary Figs. 22, 23, and 24). Prior probabilities were set proportional to the occurrence of each mark type in the dataset (see Supplementary Code 1).

Final determination of cut marks. Any BSM suspected to be anthropic in nature was analyzed both qualitatively and quantitatively. For the qualitative analysis, we recorded the characteristics as described above for linear marks (following¹⁸). Molds of each mark were made and quantitatively analyzed as described above by MP. For these, results included a prior probability that each mark fell into a given category. Some marks were only assessed qualitatively because they were unable to be molded (or scans of the molds failed) or the molds themselves did not pick up the marks in question.

All qualitative and quantitative data were then consolidated and examined collectively by the research team and determinations made regarding the anthropogenic nature of each mark. Linear marks were placed into one of three categories based on their qualitative attributes and results of the quantitative analyses: 1) high-confidence cut marks, 2) probable cut marks, and 3) an “unknown marks” group. High-confidence cut marks were defined as those presenting most of the qualitative characteristics of cut marks as defined by Domínguez-Rodrigo et al.¹⁹ and most were categorized as cut marks in the quantitative analysis. Probable cut marks were those that presented multiple qualitative characteristics indicative of cut marks but were less consistently identified as cut marks in the quantitative analysis or were not analyzed. Unknown marks are those that are not consistent with other taphonomic agents (e.g., trampling, tooth marks) and presented some qualitative characteristics of cut marks but did not include enough characteristics for our team to confidently assign them as anthropogenic in origin. When our qualitative and quantitative analyses returned conflicting results on the nature of the marks, the qualitative analysis was given higher weight due to the holistic nature of our analysis.

U-Pb dating methods. We specifically chose dental samples for U-Pb analysis that would not be useful for other taxonomic assessments (e.g., isolated or fragmentary teeth). Because evidence suggests that the site of Grăunceanu represents a single depositional event, sampling of specimens from this site is essentially random in nature and therefore results should be representative of the entire accumulation. Samples for U-Pb dating were mounted in resin blocks, polished down to reveal internal structures (Supplementary Fig. 25) and arranged in the S155 large-format ablation cell of an Applied Spectra RESOLUTION-SE ablation system based around an ATL Atlex 193 nm excimer laser. A beam expander was employed for any laser spots above 200 microns. This sample introduction system was coupled to a Nu Instruments Attom-ES high resolution magnetic sector ICP-MS operating in deflector jump mode. Analytical methods follow those outlined for carbonate materials in Woodhead & Petrus²¹; details of instrumental parameters are found in Supplementary Table 2.

Laser fluence was typically adjusted to $\sim 2\text{--}3\text{ J cm}^{-2}$, with a laser repetition rate of 5 Hz. Spot sizes were highly variable in the range 20–200 microns dependent upon sample U contents, which were also highly variable. Tuning of laser gas flows and lenses aimed to achieve maximum Pb counts, without taking ^{238}U into attenuated mode (3 million cps). Low oxide levels ($^{248}\text{ThO}/^{232}\text{Th} < 0.3\%$) were preferred but no effort was made to tune to Th/U = 1 as is common practice in some trace element studies. A brief pre-ablation using a larger spot size was conducted prior to every analysis. Baseline measurement for 30 s was followed by 40 s acquisition during each spot ablation.

Two different primary standards were employed. For most analyses we used a relatively homogeneous ‘in house’ apatite standard ‘BR-13’ but for materials with low U content this was not always possible without tripping the detector into attenuation mode for the calibration standard; for such samples we calibrated using the McClure apatite⁶⁰. A variety of apatite secondary standards were employed in the course of this study including Kovdor⁶¹, Durango⁶², and ‘401’⁶³. All produced ages within 1% of reference values providing confidence in the accuracy of our methods.

Initial data reduction was performed using the VizualAge UcomPbine data reduction scheme (DRS⁶⁴) for Lolite, a popular ICPMS data processing software package⁶⁵ which is designed to allow the use of heterogeneous reference materials (i.e. those with variable amounts of common Pb such as McClure apatite but assumes no $^{207}\text{Pb}/^{206}\text{Pb}$ fractionation). The time-resolved reference material data from a single spot analysis exhibit shifts in $^{238}\text{U}/^{206}\text{Pb}$ – $^{207}\text{Pb}/^{206}\text{Pb}$ isochron space primarily from encountering variably common Pb and/or experiencing downhole Pb/U fractionation. UcomPbine corrects each time slice of background-subtracted data for the reference material based on its known common and radiogenic Pb compositions using a ^{204}Pb – ^{207}Pb – ^{208}Pb -based approach (the ^{207}Pb based correction was used in this study). Drift correction is carried out as usual in Lolite by fitting a function (in this case a smoothing spline) to the reference material analyses that bracket unknowns.

$^{238}\text{U}/^{234}\text{U}$ measurements were undertaken following the procedure of Hellstrom⁶⁶ as modified by Drysdale et al.⁶⁷. Initially, relatively large samples of 2–3 mg were drilled from six teeth which returned successful U-Pb isochrons, using a tungsten carbide dental bit. These were dissolved in concentrated HNO_3 , dried down and re-dissolved in 1.0 ml of 5 % HNO_3 / 0.5 % HF, 0.01 ml aliquots of which were further diluted in the same acid to 0.8 ml, spiked with a mixed ^{229}Th – ^{233}U – ^{236}U tracer and equilibrated on a hotplate overnight. These were introduced directly to a Nu Instruments Plasma MC-ICP-MS and measured using a mass jumping routine using mixed Faraday cups and secondary electron multipliers. The procedure was repeated on a second aliquot of each sample, giving inconsistent $^{230}\text{Th}/^{238}\text{U}$ ratios but good replication of $^{234}\text{U}/^{238}\text{U}$.

An insoluble organic microparticulate Th-bearing fraction was inferred to be present in the bulk solutions, invalidating $^{230}\text{Th}/^{238}\text{U}$ measurements on spiked aliquots of dissolved samples, so all teeth were resampled using a 350 μm tungsten carbide microdrill to a depth of 350 μm giving samples of approximately 75 μg (equivalent to $\sim 10\text{--}100\text{ ng U}$). These were dissolved in concentrated HNO_3 and refluxed overnight before addition of 5 drops of conc H_2O_2 to oxidize the inferred insoluble organic phase, with effervescence observed. Samples were then dried down and redissolved in 0.8 ml of 5 % HNO_3 / 0.5 % HF, spiked and equilibrated and analyzed as above.

Corrections for initial isotopic disequilibrium in $^{234}\text{U}/^{238}\text{U}$ and final isochron construction was performed using DQPB software⁶⁸, and the robust isochron fitting technique described by Powell et al.⁶⁸ and Monte Carlo uncertainty propagation employing 50,000 iterations.

Stable isotope analysis. Enamel powder from the upper cheek teeth series ($\text{P}^2\text{--M}^2$) of an *Equus sp.* specimen (VGr.0974) was sampled sequentially along the growth layers using a dental drill, at a resolution of 1.5–2.5 mm, after removing the cementum. Stable isotopes of oxygen and carbon in the structural carbonate of the third molar (M^2) were analyzed at the University of Arkansas Stable Isotope Laboratory, USA (UASIL), while the premolars ($\text{P}^2\text{--P}^4$) and the remaining molars ($\text{M}^1\text{--M}^2$) were analyzed at the University of Northumbria, UK. Both laboratories use Thermo Delta V Advantage isotope ratio mass spectrometers coupled to GasBench II sample preparation devices. Prior to analysis, samples were treated with 1M acetic acid, rinsed with deionized water, and dried.

The Northumbria University stable isotope laboratory uses an analysis method adapted from Spötl and Venneman⁶⁹. $2000 \pm 20\ \mu\text{g}$ of sample were loaded into 12 mL borosilicate vials capped with butyl rubber septa (LabcoTM), and flushed with helium for 480 s at 1.8 bar on a bespoke flushing box supplied by Sercon Ltd. Carbon. Individual measurement sequences (‘runs’) consisted of 80 measurements, including standards, and all samples were reacted with 102 wt% orthophosphoric acid at a temperature of 70 °C, with a reaction time of 104 min prior to measurement to ensure equilibration. For data evaluation, standards were measured at the beginning, end, and approximately every 10 samples in each run. An in-house laboratory calcite standard (Plessen) was used for linearity and drift correction

($\delta^{13}\text{C} = 2.40\text{‰}$, $\delta^{18}\text{O} = -1.31\text{‰}$, $n = 10$ per run), alongside international standards NBS18 and IAEA603 for stretching correction (each $n \geq 3$ per run). Nominal values from Kim et al.⁷⁰ were used for NBS18 ($\delta^{13}\text{C} = -5.01\text{‰}$, $\delta^{18}\text{O} = -23.01\text{‰}$), while values stated by the IAEA were used for IAEA603 (www.iaea.org; $\delta^{13}\text{C} = 2.46\text{‰}$, $\delta^{18}\text{O} = -2.37\text{‰}$). One sample of an in-house calcite standard (PoI2, $\delta^{13}\text{C} = -7.14\text{‰}$, $\delta^{18}\text{O} = -9.22\text{‰}$) was added to each run and used to evaluate long-term performance. Based on this secondary standard, for the measurement period relevant to the samples reported here, reproducibility is better than 0.1‰ for both $\delta^{13}\text{C}$ and $\delta^{18}\text{O}$. All stable isotope data was initially reported on the VPDB scale, but for climate calculations $\delta^{18}\text{O}$ values were transferred to the VSMOW scale using the equation $\delta^{18}\text{O}_{(\text{VSMOW})} = \delta^{18}\text{O}_{(\text{VPDB})} \times 1.03092 + 30.92$ ⁷⁰.

At UASIL, an international standard (NBS19) and an in-house standard (UASIL 22) were used for corrections, each in 8 aliquots analyzed during the entire run. NBS19 standard values are $\delta^{13}\text{C} = 1.95\text{‰}$ VPDB, $\delta^{18}\text{O} = 28.72\text{‰}$ VSMOW, while UASIL 22 values are $\delta^{13}\text{C} = -35.6\text{‰}$ VPDB, $\delta^{18}\text{O} = 13.31\text{‰}$ VSMOW. The standard deviation values for NBS19 and UASIL 22 during the analysis of this set of samples were $\delta^{13}\text{C} - 0.09\text{‰}$ and $\delta^{18}\text{O} - 0.17\text{‰}$, and $\delta^{13}\text{C} - 0.08\text{‰}$ and $\delta^{18}\text{O} - 0.13\text{‰}$, respectively.

Oxygen stable isotopes in the phosphate component of the enamel of M^3 were analyzed at UASIL in six samples and reported on the VSMOW scale. The phosphate was precipitated as Ag_3PO_4 and analyzed in a Thermo Delta V Advantage IRMS coupled to a TC-EA. Four standards were measured along with this batch of samples: NIST 120c, USGS 80, USGS 81, and an in-house Ag_3PO_4 standard, with values of 21.93‰, 13.12‰, 34.78‰, and 6.57‰ VSMOW respectively. Their within-run standard deviation values were 0.60‰, 0.37‰, 0.54‰, and 0.29‰.

Average $\delta^{18}\text{O}$ values for each tooth were calculated considering that summer season is defined by more data points than winter, thus including all of them in the calculation of the average would skew the result to higher values. To solve this issue, for each tooth we used the same number of samples from summer as there were in winter. For example, P^3 has 15 data points from two summer seasons while the full winter season is clearly defined by only 7 points. We eliminated from the calculation of the average the summer data points from both ends of the series until we were left with 7 data points. By contrast, P^2 winter is defined by four data points, whereas the summer is defined by only two, leading us to include only two winter values in the calculation.

Using the available $\delta^{18}\text{O}_{\text{PO}_4}$ and $\delta^{18}\text{O}_{\text{CaCO}_3}$ values, we calculated the relationship between them as $\delta^{18}\text{O}_{\text{PO}_4} = \delta^{18}\text{O}_{\text{CaCO}_3} \times 0.96 - 8.06$ (after rejecting one data point as an outlier), similar to the equation of lacumin et al.⁷¹ ($\delta^{18}\text{O}_{\text{PO}_4} = \delta^{18}\text{O}_{\text{CaCO}_3} \times 0.98 - 8.5$). The shift between our measured $\text{PO}_4\text{-CO}_3$ samples is on average 8.9‰, also similar to the lacumin et al. value of 9.1‰, indicating little to no diagenesis. We therefore have high confidence that diagenetic changes are not meaningfully influencing our results. Because the lacumin et al. equation is based on a larger dataset, we used that equation to calculate equivalent $\delta^{18}\text{O}_{\text{PO}_4}$ values for the entire data series of $\delta^{18}\text{O}_{\text{CaCO}_3}$ and further, we used the equations $\delta^{18}\text{O}_{\text{PO}_4} = \delta^{18}\text{O}_{\text{H}_2\text{O}} \times 0.71 + 22.60$ of Huertas et al.²², $\delta^{18}\text{O}_{\text{PO}_4} = \delta^{18}\text{O}_{\text{H}_2\text{O}} \times 0.9 + 23$ of Kohn and Cerling²⁴, and $\delta^{18}\text{O}_{\text{H}_2\text{O}} = \delta^{18}\text{O}_{\text{PO}_4} \times 1.11 - 26.44$ of Amiot et al.²³ to calculate $\delta^{18}\text{O}$ values of local meteoric water. Of these equations, only Amiot et al. incorporates error estimates; these errors are given as $\delta^{18}\text{O}_w = 1.1128 (\pm 0.0029) \times \delta^{18}\text{O}_{\text{PO}_4} - 26.4414 (\pm 0.0508)$. However, integrating those uncertainties would affect only the second digit of the results, with no discernible change in our interpretation.

While enamel $\delta^{13}\text{C}$ values are generally shifted by $14.1 \pm 0.5\text{‰}$ compared to plants⁷², we calculated the average annual plant value and corrected it for the difference of 1.7‰ between modern and Quaternary atmospheric CO_2 ⁷³. The resulting plant tissue value was then used in the equation of Kohn²⁹, which allows for the calculation of the mean annual precipitation amount (MAP): $\delta^{13}\text{C}(\text{‰}, \text{VPDB}) = -10.29 + 1.90 \times 10^{-4} \times \text{altitude (m)} - 5.61 \times \log_{10}(\text{MAP} + 300, \text{mm/year}) - 0.0124 \times \text{latitude (°)}$,

where the altitude of our site is 300 m and latitude is 45°. Kohn and McKay⁷⁴ estimate the uncertainties of this equation as being ~50% for MAP values higher than 500 mm/year, but never decreased below 120 mm/year. Although Kohn²⁹'s equation is intended to calculate annual precipitation values, we divide the results into 12 months in order to calculate monthly values (as described in the SI). To our knowledge, such use of this equation has not been validated before.

Reporting summary

Further information on research design is available in the Nature Portfolio Reporting Summary linked to this article.

Data availability

All data are available in the main text, supplementary discussion, and supplementary data. Fossil materials are housed at the "Emil Racoviță" Institute of Speleology (ISER) in Bucharest, Romania and the Museum of Oltenia (MO) in Craiova, Romania; access to these collections can be requested by contacting coauthors Petculescu (ISER) and/or Popescu (MO). Source Data for Figs. 1, 3, 4, and 5 can be found in the Supplementary Data files. Comparative data from the quantitative analysis of the cut marks is available upon request to Michael Pante.

Code availability

All software and code used for data collection and analysis are outlined in the methods section of the manuscript or provided in Supplementary Code 1.

References

- Ferring, R. et al. Earliest human occupations at Dmanisi (Georgian Caucasus) dated to 1.85–1.78 Ma. *P Natl Acad. Sci. USA* **108**, 10432–10436 (2011).
- Lordkipanidze, D. et al. A complete skull from Dmanisi, Georgia, and the evolutionary biology of early. *Science* **342**, 326–331 (2013).
- Tappen, M., Bukhsianidze, M., Ferring, R., Coil, R. & Lordkipanidze, D. Life and death at Dmanisi, Georgia: taphonomic signals from the fossil mammals. *J. Hum. Evol.* **171**, 103249 (2022).
- Dennell, R. Dispersal and colonisation, long and short chronologies: How continuous is the Early Pleistocene record for hominids outside East Africa? *J. Hum. Evol.* **45**, 421–440 (2003).
- Muttoni, G., Scardia, G. & Kent, D. V. Early hominins in Europe: The Galerian migration hypothesis. *Quat. Sci. Rev.* **180**, 1–29 (2018).
- Key, A. & Ashton, N. Hominins likely occupied northern Europe before one million years ago. *Evol. Anthropol.* **32**, 10–25 (2023).
- Zhu, Z. Y. et al. Hominin occupation of the Chinese Loess Plateau since about 2.1 million years ago. *Nature* **559**, 608–612 (2018).
- Andresescu, I. et al. New developments in the upper Pliocene–Pleistocene stratigraphic units of the Dacian Basin (Eastern Paratethys), Romania. *Quatern Int* **284**, 15–29 (2013).
- Radulesco, C. & Samson, P. The Plio–Pleistocene mammalian succession of the Olteț Valley, Dacic Basin, Romania. *Quartärpaläontologie* **8**, 225–232 (1990).
- Bolomey, A. Die fauna zweier villafrankischer fundstellen in rumänien: vorläufige mitteilungen. *Ber. der Geologischen Ges., DDR* **10**, 77–88 (1965).
- Terhune, C. E. et al. Early Pleistocene fauna of the Olteț River Valley of Romania: Biochronological and biogeographic implications. *Quatern Int* **553**, 14–33 (2020).
- Croitore, R. et al. Early Pleistocene ruminants (Artiodactyla, Mammalia) from the Dacian Basin (South Romania) before and after the event: Implications for hominin dispersals in Western Eurasia. *Hist Biol*, 485–533. <https://doi.org/10.1080/08912963.2023.2167602> (2024).
- Terhune, C. E., Gaudin, T., Curran, S. & Petculescu, A. The youngest pangolin (Mammalia, Pholidota) from Europe. *J. Vertebr. Paleontol.* **41**, e1990075 (2021).

14. Werdelin, L. et al. Carnivora from the early Pleistocene of Grăunceanu (Olteț River Valley, Dacian Basin, Romania). *Riv. Ital. Paleontol. S* **129**, 457–476 (2023).
15. Curran, S. et al. Multiproxy paleoenvironmental reconstruction of Early Pleistocene sites from the Olteț River Valley of Romania. *Palaeogeogr. Palaeoclimatol.* **574**, 110445 (2021).
16. Radulesco, C., Samson, P.-M. & Stiuca, E. Biostratigraphic framework of the Lower Paleolithic in Romania. *Quaternaire* **9**, 283–290 (1998).
17. Blumenschine, R. J., Marean, C. W. & Capaldo, S. D. Blind tests of inter-analyst correspondence and accuracy in the identification of cut marks, percussion marks, and carnivore tooth marks on bone surfaces. *J. Archaeol. Sci.* **23**, 493–507 (1996).
18. Domínguez-Rodrigo, M., de Juana, S., Galán, A. B. & Rodríguez, M. A new protocol to differentiate trampling marks from butchery cut marks. *J. Archaeol. Sci.* **36**, 2643–2654 (2009).
19. Domínguez-Rodrigo, M., Pickering, T. R. & Bunn, H. T. Configurational approach to identifying the earliest hominin butchers. *P Natl Acad. Sci. USA* **107**, 20929–20934 (2010).
20. Pante, M. C. et al. A new high-resolution 3-D quantitative method for identifying bone surface modifications with implications for the Early Stone Age archaeological record. *J. Hum. Evol.* **102**, 1–11 (2017).
21. Woodhead, J. & Petrus, J. A. Exploring the advantages and limitations of in situ U-Pb carbonate geochronology using speleothems. *Geochronology* **1**, 69–84 (2019).
22. Huertas, A. D., Iacumin, P., Stenni, B., Chillon, B. S. & Longinelli, A. Oxygen-Isotope variations of phosphate in mammalian bone and tooth enamel. *Geochim Cosmochim. Acta* **59**, 4299–4305 (1995).
23. Amiot, R. et al. Latitudinal temperature gradient during the Cretaceous Upper Campanian-Middle Maastrichtian: δO record of continental vertebrates. *Earth Planet. Sc. Lett.* **226**, 255–272 (2004).
24. Kohn, M. J. & Cerling, T. E. Stable isotope compositions of biological apatite. *Rev. Miner. Geochem* **48**, 455–488 (2002).
25. Rozanski, K., Araguás-Araguás, L. & Gonfiantini, R. in *Geophysical Monograph Series Vol. 78* (eds P. K. Swart, K. C. Lohmann, J. McKenzie, & S. Savin) 1–36 (1993).
26. Pryor, A. J. E., Stevens, R. E., O’Connell, T. C. & Lister, J. R. Quantification and propagation of errors when converting vertebrate biomineral oxygen isotope data to temperature for palaeoclimate reconstruction. *Palaeogeogr. Palaeoclimatol.* **412**, 99–107 (2014).
27. IAEA/WMO. Global Network of Isotopes in Precipitation (GNIP) database. <https://nucleus.iaea.org/wiser> (2023).
28. Domingo, L. et al. Late Neogene and Early Quaternary paleoenvironmental and paleoclimatic conditions in southwestern Europe: Isotopic analyses on mammalian taxa. *Plos One* **8**, e63739 (2013).
29. Kohn, M. J. Carbon isotope compositions of terrestrial C3 plants as indicators of (paleo)ecology and (paleo)climate. *Proc. Natl. Acad. Sci. USA* **107**, 19691–19695 (2010).
30. Scardia, G. et al. Chronologic constraints on hominin dispersal outside Africa since 2.48 Ma from the Zarqa Valley, Jordan. *Quat. Sci. Rev.* **219**, 1–19 (2019).
31. Malassé, A. D. et al. Intentional cut marks on bovid from the Quranwala zone, 2.6 Ma, Siwalik Frontal Range, northwestern India. *Cr. Palevol* **15**, 317–339 (2016).
32. Sablin, M. V. & Giry, E. Y. The earliest evidence of human occupation in southeastern Europe: a processed camel bone fragment from the Lower Don. *Archaeol., Ethnol. Anthropol. Eurasia* **38**, 7–13 (2010).
33. Sablin, M. V. & Iltsevich, K. Faunal complex of the Early Pleistocene Muhkai 2 locality. *Proc. Zool. Inst. RAS* **325**, 82–90 (2021).
34. Li, H., Li, C. R. & Kuman, K. Longgudong, an Early Pleistocene site in Jianshi, South China, with stratigraphic association of human teeth and lithics. *Sci. China Earth Sci.* **60**, 452–462 (2017).
35. Toro-Moyano, I. et al. The oldest human fossil in Europe, from Orce (Spain). *J. Hum. Evol.* **65**, 1–9 (2013).
36. Lebatard, A. E. et al. Dating the *Homo erectus* bearing travertine from Kocabas (Denizli, Turkey) at at least 1.1 Ma. *Earth Planet. Sc. Lett.* **390**, 8–18 (2014).
37. Carbonell, E. et al. The first hominin of Europe. *Nature* **452**, 465–467 (2008).
38. Sahnouni, M. et al. The first evidence of cut marks and usewear traces from the Plio-Pleistocene locality of El-Kherba (Ain Hanech), Algeria: implications for early hominin subsistence activities circa 1.8 Ma. *J. Hum. Evol.* **64**, 137–150 (2013).
39. Sahnouni, M. et al. 1.9-million- and 2.4-million-year-old artifacts and stone tool-cutmarked bones from Ain Boucherit, Algeria. *Science* **362**, 1297–1301 (2018).
40. Huguet, R. et al. Level TE9c of Sima del Elefante (Sierra de Atapuerca, Spain): a comprehensive approach. *Quatern Int* **433**, 278–295 (2017).
41. Barr, W. A., Pobiner, B., Rowan, J., Du, A. & Faith, J. T. No sustained increase in zooarchaeological evidence for carnivory after the appearance of *Homo erectus*. *P Natl Acad. Sci. USA* **119**, e2115540119 (2022).
42. Pobiner, B. L., Rogers, M. J., Monahan, C. M. & Harris, J. W. K. New evidence for hominin carcass processing strategies at 1.5 Ma, Koobi Fora, Kenya. *J. Hum. Evol.* **55**, 103–130 (2008).
43. Thompson, J. C. et al. Taphonomy of fossils from the hominin-bearing deposits at Dikika, Ethiopia. *J. Hum. Evol.* **86**, 112–135 (2015).
44. Cáceres, I., Semaw, S., Rogers, M. J. & Leiss, A. C. Hominin exploitation of animal resources in the Gona Pleistocene archaeological sites (Afar, Ethiopia). In *Proc. II Meeting of African Prehistory 199–217* (CENIEH, 2015).
45. Leakey, M. G. et al. New fossils from Koobi Fora in northern Kenya confirm taxonomic diversity in early *Homo*. *Nature* **488**, 201–204 (2012).
46. Herries, A. I. R. et al. Contemporaneity of *Australopithecus*, *Paranthropus*, and early *Homo erectus* in South Africa. *Science* **368**, eaaw7293 (2020).
47. Mussi, M. et al. Early *Homo erectus* lived at high altitudes and produced both Oldowan and Acheulean tools. *Science* **382**, 713–718 (2023).
48. O’Regan, H. J., Bishop, L. C., Elton, S., Lamb, A. L. & Turner, A. Afro-Eurasian mammalian dispersal routes of the Late Pliocene and Early Pleistocene, and their bearing on earliest hominin movements. *Cour. Forsch.-Inst. Senckenberg* **256**, 305–314 (2006).
49. Garba, R. et al. East-to-west human dispersal into Europe 1.4 million years ago. *Nature*, 1–6. <https://doi.org/10.1038/s41586-024-07151-3> (2024).
50. Derricourt, R. Getting “Out of Africa”: Sea crossings, land crossings and culture in the hominin migrations. *J. World Prehist.* **19**, 119–132 (2005).
51. Krijgsman, W. et al. Quaternary time scales for the Pontocaspian domain: interbasinal connectivity and faunal evolution. *Earth-Sci. Rev.* **188**, 1–40 (2019).
52. Potts, R. Environmental hypotheses of hominin evolution. *Yearb. Phys. Anthropol.* **41**, 93–136 (1998).
53. Keevil, T. *Inferring early stone age tool technology and raw material from cut mark micromorphology using high-resolution 3-D scanning with applications to middle bed II, Olduvai Gorge, Tanzania* MA thesis, Colorado State University, (2018).
54. Muttart, M. V. *Taxonomic distinctions in the 3D micromorphology of tooth marks with application to feeding traces from middle bed II, Olduvai Gorge, Tanzania* MA thesis, Colorado State University, (2017).
55. Orlikoff, E., Keevil, T. & Pante, M. in *Paleoanthropology Society* (Vancouver, BC, 2017).
56. Tolley, A., Pante, M., de la Torre, I., Njau, J. K. & McHenry, L. in *Paleoanthropology Society* (Albuquerque, NM, 2019).

57. Venables, W. & Ripley, B. *Modern Applied Statistics with S*. Fourth edn, (Springer, 2002).
 58. Friedman, J. H. Regularized Discriminant-Analysis. *J. Am. Stat. Assoc.* **84**, 165–175 (1989).
 59. R: A language and environment for statistical computing (R Foundation for Statistical Computing, Vienna, Austria, 2021).
 60. Schoene, B. & Bowring, S. A. U-Pb systematics of the McClure Mountain syenite: thermochronological constraints on the age of the $^{40}\text{Ar}/^{39}\text{Ar}$ standard MMhb. *Contrib. Miner. Petr.* **151**, 615–630 (2006).
 61. Amelin, Y. & Zaitsev, A. N. Precise geochronology of phoscorites and carbonatites: the critical role of U-series disequilibrium in age interpretations. *Geochim Cosmochim. Acta* **66**, 2399–2419 (2002).
 62. McDowell, F. W., McIntosh, W. C. & Farley, K. A. A precise ^{40}Ar - ^{39}Ar reference age for the Durango apatite (U-Th)/He and fission-track dating standard. *Chem. Geol.* **214**, 249–263 (2005).
 63. Thompson, J. et al. Matrix effects in Pb/U measurements during LA-ICP-MS analysis of the mineral apatite. *J. Anal. At. Spectrom.* **31**, 1206–1215 (2016).
 64. Chew, D. M., Petrus, J. A. & Kamber, B. S. U-Pb LA-ICPMS dating using accessory mineral standards with variable common Pb. *Chem. Geol.* **363**, 185–199 (2014).
 65. Paton, C., Hellstrom, J., Paul, B., Woodhead, J. & Hergt, J. Iolite: freeware for the visualisation and processing of mass spectrometric data. *J. Anal. At. Spectrom.* **26**, 2508–2518 (2011).
 66. Hellstrom, J. Rapid and accurate U/Th dating using parallel ion-counting multi-collector ICP-MS. *J. Anal. At. Spectrom.* **18**, 1346–1351 (2003).
 67. Drysdale, R. N. et al. Precise microsampling of poorly laminated speleothems for U-series dating. *Quat. Geochronol.* **14**, 38–47 (2012).
 68. Pollard, T. et al. DQPB: software for calculating disequilibrium U-Pb ages. *Geochronology* **5**, 181–196 (2023).
 69. Spötl, C. & Vennemann, T. W. Continuous-flow isotope ratio mass spectrometric analysis of carbonate minerals. *Rapid Commun. Mass Sp.* **17**, 1004–1006 (2003).
 70. Kim, S. T., Coplen, T. B. & Horita, J. Normalization of stable isotope data for carbonate minerals: Implementation of IUPAC guidelines. *Geochim Cosmochim. Acta* **158**, 276–289 (2015).
 71. Iacumin, P., Bocherens, H., Mariotti, A. & Longinelli, A. Oxygen isotope analyses of co-existing carbonate and phosphate in biogenic apatite: A way to monitor diagenetic alteration of bone phosphate? *Earth Planet. Sc. Lett.* **142**, 1–6 (1996).
 72. Cerling, T. E. & Harris, J. M. Carbon isotope fractionation between diet and bioapatite in ungulate mammals and implications for ecological and paleoecological studies. *Oecologia* **120**, 347–363 (1999).
 73. Tipple, B. J., Meyers, S. R. & Pagani, M. Carbon isotope ratio of Cenozoic CO₂: a comparative evaluation of available geochemical proxies. *Paleoceanography* **25**. <https://doi.org/10.1029/2009PA001851> (2010).
 74. Kohn, M. J. & McKay, M. P. Paleoeology of late Pleistocene-Holocene faunas of eastern and central Wyoming, USA, with implications for LGM climate models. *Palaeogeogr. Palaeoclimatol.* **326**, 42–53 (2012).
 75. Hoppe, K. A., Stover, S. M., Pascoe, J. R. & Amundson, R. Tooth enamel biomineralization in extant horses: implications for isotopic microsampling. *Palaeogeogr. Palaeoclimatol.* **206**, 355–365 (2004).
- Dana Stamatiou, Cristina Stan, Emil Ştiucă, Ioan Tanţău, Peter Ungar, Laura Văcărescu, and Caitlin Yoakum. We especially thank the people of the Olteţ Valley and Tetoiu for their assistance during fieldwork and for initially locating many of these fossils. We acknowledge the following funding sources: The Leakey Foundation (SC, CT, BP, VD, APe, CR); National Science Foundation grant BCS-1636686 (CT, SC, APe, CR); The Josiah Charles Trent Foundation and Duke University (CT); The University of Arkansas (CT); Ohio University (SC); The University of California Santa Barbara (SC); The Peter Buck Fund for Human Origins Research (BP); Romanian Ministry of Education and Research, CNCS - UEFISCDI, project number PN-III-P4-ID-PCE-2020-2282 (ECHOES) (VD); Australian Research Council (JW). This manuscript was improved by comments from editor Devin Ward and four peer reviewers.

Author contributions

Conceptualization: S.C., C.T., C.R., B.P., A.Pe., V.D.; Methodology: S.C., C.T., B.P., V.D., J.H., J.W., M.P.; Investigation: S.C., B.P., S.G., V.D., M.P., J.H., J.W., R.C., A.D., V.E., A.Po., C.R., L.W., A.Pe., C.T.; Formal Analysis: S.C., C.T., B.P., M.P., V.D., J.H., J.W., V.E., T.K.; Visualization: C.T., V.D., S.C., M.P., J.H., J.W., A.D.; Data Curation: A.Po., A.Pe., C.T., S.C., V.D.; Resources: A.Pe., Apo; Funding acquisition: C.T., S.C., C.R., B.P., V.D., Ape; Project administration: CT, SC; Writing – original draft: S.C., C.T., V.D., M.P., J.H., J.W., BP; Writing – review & editing: S.C., B.P., S.G., V.D., M.P., J.H., J.W., R.C., A.D., V.E., T.K., A.Po., C.R., L.W., A.Pe., C.T.

Competing interests

Authors declare that they have no competing interests.

Additional information

Supplementary information The online version contains supplementary material available at <https://doi.org/10.1038/s41467-025-56154-9>.

Correspondence and requests for materials should be addressed to Sabrina C. Curran or Claire E. Terhune.

Peer review information *Nature Communications* thanks Lloyd Courtenay, Mathieu Duval and the other, anonymous, reviewer(s) for their contribution to the peer review of this work. A peer review file is available.

Reprints and permissions information is available at <http://www.nature.com/reprints>

Publisher's note Springer Nature remains neutral with regard to jurisdictional claims in published maps and institutional affiliations.

Open Access This article is licensed under a Creative Commons Attribution-NonCommercial-NoDerivatives 4.0 International License, which permits any non-commercial use, sharing, distribution and reproduction in any medium or format, as long as you give appropriate credit to the original author(s) and the source, provide a link to the Creative Commons licence, and indicate if you modified the licensed material. You do not have permission under this licence to share adapted material derived from this article or parts of it. The images or other third party material in this article are included in the article's Creative Commons licence, unless indicated otherwise in a credit line to the material. If material is not included in the article's Creative Commons licence and your intended use is not permitted by statutory regulation or exceeds the permitted use, you will need to obtain permission directly from the copyright holder. To view a copy of this licence, visit <http://creativecommons.org/licenses/by-nc-nd/4.0/>.

© The Author(s) 2025

Acknowledgements

Thank you to the following people helped with data collection, fieldwork, and provided advice: Eric Delson, Kieran McNulty, Viorel Horoi, Silviu Constantin, Marius Robu, Martha Tappen, Răzvan Arghir, Amber Cooper, David Fox, Niki Garrett, Timothy Gaudin, Jenifer Hubbard, Lydia B. Ironside, Eric Mazelis, Ionuţ Mirea, Ipyana Mwakyoma, Ashly Romero,